Phytoplankton diversity and chemotaxonomy in contrasting North Pacific ecosystems (#74249)

First submission

Guidance from your Editor

Please submit by **27 Jun 2022** for the benefit of the authors (and your $200 publishing discount) .

Structure and Criteria
Please read the 'Structure and Criteria' page for general guidance.

Raw data check
Review the raw data.

Image check
Check that figures and images have not been inappropriately manipulated.

Privacy reminder: If uploading an annotated PDF, remove identifiable information to remain anonymous.

Files

Download and review all files from the materials page.

6 Figure file(s)
8 Table file(s)
3 Raw data file(s)

Structure your review

The review form is divided into 5 sections. Please consider these when composing your review:

1. **BASIC REPORTING**
2. **EXPERIMENTAL DESIGN**
3. **VALIDITY OF THE FINDINGS**
4. General comments
5. Confidential notes to the editor

You can also annotate this PDF and upload it as part of your review

When ready submit online.

Editorial Criteria

Use these criteria points to structure your review. The full detailed editorial criteria is on your guidance page.

BASIC REPORTING

- Clear, unambiguous, professional English language used throughout.
- Intro & background to show context. Literature well referenced & relevant.
- Structure conforms to PeerJ standards, discipline norm, or improved for clarity.
- Figures are relevant, high quality, well labelled & described.
- Raw data supplied (see PeerJ policy).

EXPERIMENTAL DESIGN

- Original primary research within Scope of the journal.
- Research question well defined, relevant & meaningful. It is stated how the research fills an identified knowledge gap.
- Rigorous investigation performed to a high technical & ethical standard.
- Methods described with sufficient detail & information to replicate.

VALIDITY OF THE FINDINGS

- Impact and novelty not assessed. *Meaningful* replication encouraged where rationale & benefit to literature is clearly stated.
- All underlying data have been provided; they are robust, statistically sound, & controlled.
- Conclusions are well stated, linked to original research question & limited to supporting results.

Standout reviewing tips

The best reviewers use these techniques

Tip	*Example*
Support criticisms with evidence from the text or from other sources	*Smith et al (J of Methodology, 2005, V3, pp 123) have shown that the analysis you use in Lines 241-250 is not the most appropriate for this situation. Please explain why you used this method.*
Give specific suggestions on how to improve the manuscript	*Your introduction needs more detail. I suggest that you improve the description at lines 57- 86 to provide more justification for your study (specifically, you should expand upon the knowledge gap being filled).*
Comment on language and grammar issues	*The English language should be improved to ensure that an international audience can clearly understand your text. Some examples where the language could be improved include lines 23, 77, 121, 128 – the current phrasing makes comprehension difficult. I suggest you have a colleague who is proficient in English and familiar with the subject matter review your manuscript, or contact a professional editing service.*
Organize by importance of the issues, and number your points	*1. Your most important issue* *2. The next most important item* *3. …* *4. The least important points*
Please provide constructive criticism, and avoid personal opinions	*I thank you for providing the raw data, however your supplemental files need more descriptive metadata identifiers to be useful to future readers. Although your results are compelling, the data analysis should be improved in the following ways: AA, BB, CC*
Comment on strengths (as well as weaknesses) of the manuscript	*I commend the authors for their extensive data set, compiled over many years of detailed fieldwork. In addition, the manuscript is clearly written in professional, unambiguous language. If there is a weakness, it is in the statistical analysis (as I have noted above) which should be improved upon before Acceptance.*

Phytoplankton diversity and chemotaxonomy in contrasting North Pacific ecosystems

Antonija Matek [1], **Sunčica Bosak** [1], **Luka Šupraha** [2, 3], **Aimee Neeley** [4], **Hrvoje Višić** [5], **Ivona Cetinić** [4, 6], **Zrinka Ljubešić** [Corresp. 1]

[1] Department of Biology, Faculty of Science, University of Zagreb, Zagreb, Croatia

[2] Department of Earth Sciences, Uppsala University, Uppsala, Sweden

[3] Department of Biosciences, Section for Aquatic Biology and Toxicology (AQUA), University of Oslo, Oslo, Norway

[4] Ocean Ecology Laboratory, NASA/Goddard Space Flight Center, Greenbelt, Maryland, United States

[5] Department of Geomicrobiology, Center for Applied Geosciences, University of Tuebingen, Tuebingen, Germany

[6] Universities Space Research Association, Columbia, Maryland, United States

Corresponding Author: Zrinka Ljubešić
Email address: zrinka.ljubesic@biol.pmf.hr

Background. Phytoplankton diversity holds great potential for application in understanding of the marine ecosystems' response to climate changes, anthropogenic pressure and their impact on the oceans. **Methods.** Phytoplankton samples for detailed quantitative, qualitative and chemotaxonomic analysis of the community composition were collected in boreal winter 2017, along transect in the North Pacific Subtropical Gyre (NPSG) and the California Current System (CCS) (Honolulu, Hawaii to Portland, Oregon). **Results.** Microscopic analyses revealed that phytoplankton community of North Pacific was mostly comprised of coccolithophores (35.5%), diatoms (25.2%) and dinoflagellates (19.5%) while cryptophytes, phytoflagellates and silicoflagellates, etc. were included in group "other" that made 19.8%. A total of 207 taxa have been determined of which: 106 diatoms, 48 coccolithophores, 41 dinoflagellates, 7 other autotrophs, 4 heterotrophs and 1 cyanobacteria. NPSG oligotrophic ecosystem had lower phytoplankton abundance and diversity in comparison to CCS eutrophic ecosystem. Furthermore, signature biomarker pigments observed by chemotaxonomy analysis correlated with characteristic taxon for each ecosystem. Divinyl chlorophyll *a* and zeaxanthin were detected in higher concentrations at the NPSG, while alloxanthin, fucoxanthin, and peridinin contributed the most to CCS. **Conclusion.** Our results show that combining microscopy counts and pigment analysis did reveal the real ecosystem diversity, so we propose using both methods in the future research of North Pacific and other large ocean ecosystems in order to collect valuable data on phytoplankton diversity.

Phytoplankton diversity and chemotaxonomy in contrasting North Pacific ecosystems

Antonija Matek [1], Sunčica Bosak [1], Luka Šupraha [2, a], Aimee Neeley [3], Hrvoje Višić [4], Ivona Cetinić [3, 5], and Zrinka Ljubešić [1]

[1] University of Zagreb, Faculty of Science, Biology, Zagreb, Croatia
[2] Department of Earth Sciences, Uppsala University, Villavägen 16, 752 36 Uppsala, Sweden
[3] Ocean Ecology Laboratory at NASA/Goddard Space Flight Center, Greenbelt, Maryland, USA
[4] Department of Geomicrobiology, Center for Applied Geosciences, University of Tuebingen, 72074 Tuebingen, Germany
[5] Universities Space Research Association, Columbia, MD, USA
[a] Present address: Department of Biosciences, Section for Aquatic Biology and Toxicology (AQUA), University of Oslo, P.O. Box 1066 Blindern, 0316 Oslo, Norway

Corresponding Author:
Zrinka Ljubešić [1]
Email address: zrinka.ljubesic@biol.pmf.hr

Abstract

Background. Phytoplankton diversity holds great potential for application in understanding of the marine ecosystems' response to climate changes, anthropogenic pressure and their impact on the oceans.

Methods. Phytoplankton samples for detailed quantitative, qualitative and chemotaxonomic analysis of the community composition were collected in boreal winter 2017, along transect in the North Pacific Subtropical Gyre (NPSG) and the California Current System (CCS) (Honolulu, Hawaii to Portland, Oregon).

Results. Microscopic analyses revealed that phytoplankton community of North Pacific was mostly comprised of coccolithophores (35.5%), diatoms (25.2%) and dinoflagellates (19.5%) while cryptophytes, phytoflagellates and silicoflagellates, etc. were included in group "other" that made 19.8%. A total of 207 taxa have been determined of which: 106 diatoms, 48 coccolithophores, 41 dinoflagellates, 7 other autotrophs, 4 heterotrophs and 1 cyanobacteria. NPSG oligotrophic ecosystem had lower phytoplankton abundance and diversity in comparison to CCS eutrophic ecosystem. Furthermore, signature biomarker pigments observed by chemotaxonomy analysis correlated with characteristic taxon for each ecosystem. Divinyl chlorophyll *a* and zeaxanthin were detected in higher concentrations at the NPSG, while alloxanthin, fucoxanthin, and peridinin contributed the most to CCS.

Conclusion. Our results show that combining microscopy counts and pigment analysis did reveal the real ecosystem diversity, so we propose using both methods in the future research of North Pacific and other large ocean ecosystems in order to collect valuable data on phytoplankton diversity.

Introduction

Phytoplankton have many important roles in the marine ecosystem: they are responsible for half of the global primary production (Otero, Álvarez-Salgado & Bode, 2020), contribute to the biogeochemical cycles by being part of the biological pump through nutrient uptake and carbon sequestration (Karl & Church., 2017), and they are at the base of majority ocean ecosystems (McQuatters-Gollop et al., 2017). Therefore, any changes in phytoplankton diversity impact the oceanic carbon cycle, nutrient uptake, and zooplankton community structure,which has an indirect effect on the whole oceanic ecosystem (Ramond et al., 2021). Consequences of global warming such as temperature increase, change in ocean circulation and stratification, acidification, and deoxygenation have an impact on the phytoplankton community. It is predicted that increases in ocean temperature and other climate induced changes will affect phytoplankton metabolic rates and growth, ultimately changing the ocean-wide phytoplankton diversity, and change in overall marine productivity (Moore et al., 2018; Cael, Dutkiewicz & Henson, 2021). Due to this expected change in phytoplankton community in the oceans of tomorrow, it is of extreme importance to understand the current baseline oceanic phytoplankton diversity and how it is shaped by environmental factors.

Oligotrophic areas of North Pacific are usually dominated by pico- and nanophytoplankton (Hoepffner & Haas, 1990; Booth, Lewin & Postel, 1993; Karl & Church., 2017; Kodama et al., 2021), while high community diversity, with presence of larger microphytoplankton (e.g. diatoms) is found in eutrophic regions of North Pacific (Almazán-Becerril, Rivas & García-Mendoza, 2012). Besides ecosystem trophic conditions, other factors can influence the phytoplankton community structure such as sharp environmental gradients, spatial distances, physical barries (Longhurst, 2007; Watson et al., 2011), and different planktonic dispersal rates (Villarino et al., 2018).

Large oceanic ecosystems, such as the North Pacific ocean are showing response to changes in climate. For instance, in autumn of 2013, a warm blob appeared in the Gulf of Alaska, and by December of 2015, it expanded toward Bering Sea, Transition Zone, and California Current System (CCS) (Peterson et al., 2016). The blob-induced increase of the sea surface temperatures had an effect on ecosystem, especially phytoplankton community structure across the whole north – east Pacific. A study done in oligotrophic North Pacific Subtropical Gyre (NPSG) by Yoon & Kim, 2020 recorded a phytoplankton community shift from nanophytoplankton to picophytoplankton during warm phases of climate oscillations when stratification is strong, and particle export is low. Moreover, in the eutrophic and diatom-dominated CCS, nutrient supply decreased for 50 % and the phytoplankton community shifted to nonsiliceous phytoplankton and/or lightly silicified diatoms (Closset et al., 2021). Long data records for North Pacific are collected at station ALOHA (22.75°N, 158°W: A Long-term Oligotrophic Habitat Assessment) in NPSG (Karl & Church., 2017) and Station M (34°50'N, 123°00'W; 4000 meters depth) in CCS ("Abyssal time-series studies at Station M"). Three decades of data from ALOHA combined with improved satellite algorithms are showing different trends of phytoplankton biomass, and net primary production growth in response to positive phases of North Pacific Gyre Oscillation, Pacific Decadal Oscillation and El Niño Southern Oscillation (Kavanaugh et al., 2018). Furthermore, two-decade record on abyssal ecosystem at station M show strong benthic-pelagic cupling, and significant response of the benthic communities to the climate induced changes in the ocean surface ("Abyssal time-series studies at Station M"). All these studies demonstrate the importance of time-series studies to record and predict future changes in ecosystems.

Recent advances in molecular and imaging technologies offer an unprecedented view of the oceanic diverstiy (Olson & Sosik, 2007; Picheral et al., 2010; "A holistic approach to marine Eco-systems biology," 2011). In a same way, chemotaxonomy offers the additional insight into the phytoplakton community structure and direct connection with remote sensing (Kramer et al., 2022). However, our vision of the phytoplankton diversity still relies on the morphological characterisation, usually done by imaging. Image based taxonomy, although often taking a lot of time, is by far the most wide-spread method in determining phytoplankton community structure, despite new automated instruments and technologies (Olson & Sosik, 2007; Picheral et al., 2010). However, this method requires a person who is trained in the discipline that is in decline (McQuatters-Gollop et al., 2017). Therefore, data presented in this paper are highly

valuable due to the lack of studies that used detailed microscopic analysis of phytoplankton performed on a wide transect in the Pacific Ocean, offering a view of taxonomically undersampled part of the ocean (Karl & Church., 2017). To fully understand the Pacific ecosystem, it is necessary to develop knowledge of the phytoplankton diversity that relates to different ecosystems, changes in environment, and can be used for future predictions of global warming's impact on marine ecosystems. Therefore, the aim of this research was to represent a true phytoplankton diversity in large marine ecosystem such as North Pacific by gathering accurate data using microscopy counts as main method, in combination with chemotaxonomy.

Materials & Methods

Expedition- location and time

Sea to Space Particle Investigation cruise aboard the Schmidt Ocean Institute R/V Falkor was conducted from January 24 to February 20, 2017, in North Pacific (Fig. 1). The North Pacific ecosystem is influenced by the Trade Winds, anticylonic North Pacific Subtropical Gyre (NPSG), and the cyclonic Subarctic Gyre that bifurcate into California Current System (CCS) and Alaska Current. The CCS is a transitional ecosystem that is more eutrophic in comparison to NPSG because of the Columiba River's contributon of terrigenous sediments and organic matter (Kammerer, 1987; Morgan, De Robertis & Zabel, 2005; Steele, Thorpe & Turekian, 2008; Kudela et al., 2010). The aim of the cruise was to connect the radiometric properties (ocean colour) with the trophic state of the ocean, and use those data to develop algorithms and phytoplankton proxies for the NASA's PACE mission (pace.oceansciences.org).

Sampling

Sampling was done along the investigated transect at Station 1 (ST1) and Station 2 (ST2) in NPSG, and Station 3 (ST3) in CCS (Fig. 1). Each station represents a group of sampling sites (Table 1) where CTD casts were deployed at three depths: the surface layer (S), deep chlorophyll maximum (DCM), and mixed layer depth (MLD), with exception at CTD 14 where additional sample was taken below mixed layer depth (BMLD) (Table 1). Samples (n=114) for phytoplankton and pigment analyses were taken by 10 L Niskin rosette sampler equipped with CTD and other sensors. For more detailed taxonomic analyses, additional samples (n=114) were taken from the same Niskin bottles, and volume of 400 mL seawater was filtered using weak vacuum onto polycarbonate filters (0.8 µm Cyclopore, 25 mm diameter, Whatman) that were placed on cellulose nitrate membranes filter (0.8 µm Whatman) to ensure an even distribution of material. The filters were rinsed with 2 mL of bottled drinking water (pH = 7.54) and dried in an oven at 50°C, and stored in dry containers for the SEM (scanning electron microscopy) analysis in the laboratory at the University of Uppsala.

For qualitative plankton analysis, another set of samples (n=27) was taken from the Niskin bottles and filtered through 20 µm mesh. Discrete phytoplankton and net phytoplankton samples were fixed with 2% neutralized formaldehyde and stored in 250 mL bottles until analyses in the laboratory of biological oceanography, Department of Biology, University of Zagreb. Four-litre triplicate seawater samples were filtered on GF/F filters for phytoplankton

pigment analysis and stored in liquid nitrogen until the high-performance liquid chromatography (HPLC) analysis in the NASA's Goddard Space Flight Center, following methods described in Hooker et al., 2012.

Phytoplankton community analysis

Light microscopy (LM) was used to determine phytoplankton composition and abundance. Subsamples of 50 or 100 mL, depending on cell density, were settled for 24 h and 48 h respectively and analyzed under a Zeiss Axiovert 200 inverted microscope using the Utermöhl method (Utermöhl, 1958). Cells larger than 20 µm were designated as microphytoplankton, and cells between 2 and 20 µm as nanophytoplankton. Typically, one transect across the counting chamber was analyzed at ×400, and two at ×200 magnification. The total count was completed at ×100 magnification for rare taxa. The minimum cell abundance that can be detected by this method is 20 cells L^{-1}. For additional taxonomic analyses, net samples were analyzed with the Zeiss Axiovert 200 inverted microscope and images of all species were taken and analyzed with Zeiss AxioVision SE64 (version 4.9.1). Micrograph plate of dominant taxa was made and edited using Adobe's Photoshop CC 2015 and Illustrator CC 2017.

Phytoplankton are comprised of a phylogenetically diverse group of both prokaryotic and eukaryotic organisms. Because of that, classification is much debated with different systematic grouping (Bray & Curtis, 2006; Roy et al., 2011; Thomas et al., 2012; Pal & Choudhury, 2014). Therefore, a simpler approach for classification will be presented in this paper with focus on morphological characteristics of most abundant forms only: cyanobacteria, diatoms, dinoflagellates, coccolithophores, cryptophytes and "others" – including phytoflagellates, silicoflagellates, ciliates and other genera. Also, phytoplankton were classified on size variation using the equivalent spherical diameter (ESD) of cells as nanophytoplankton (ESD 2–20 µm) and microphytoplankton (ESD 20–200 µm).

Trophic indices and spatial distribution

Pigment average concentrations were calculated in order to get F_p index using formula by Claustre, 1994: F_p = (sum of average concentrations of fucoxanthin and peridinin) / (sum of average concentrations of all primary pigments). Spatial distribution across investigated transects was visualized by creating one chart showing abundances of phytoplankton groups, and another one with distribution of the subset of pigments that best correlate to phytoplankton community (the correlation test explained later in Statistical analysis section). Chart plotting and calculations were made using the software Grapher 12 (GoldenSoftware) and Microsoft Office 365 ProPlus (Microsoft Corporation, version 1705), repsectively.

Statistical analysis

Several statistical analyses were done using Primer 7.0. (Primer-E Ltd 2021) to test similarities between ST1, ST2 and ST3, and correlation between phytoplankton counts and pigment data in order to gain better understanding of community diversity.

Analysis of similarity

Bray–Curtis (BC) rank similarity matrix was calculated using log(x+1) transformed data (Bray & Curtis, 2006) of phytoplankton counts. To test significance of similarity between ST1, ST2, and ST3, we run pairwise analysis of similarity (ANSOIM R statistic) on BC rank similarity matrix. Test takes averages of ranks within matrix and calculates their differences within each group in the cluster (Clarke et al., 2014). Furthermore, similarity percentages analyses (SIMPER) (Clarke, 1993) were used to observe the percentage contribution of each taxon to the average dissimilarity between samples of different groups (ST1, ST2, and ST3).

Correlation tests

In addition, another BC rank similarity matrix was calculated on log(x+1) transformed data of pigment concentrations at ST1, ST2, and ST3. We run RELATE analysis, BEST global test, and LINKTREE analyses using both BC matrices in order to test if there is a significant correlation between pigment concentrations and phytoplankton counts data.

RELATE statistic with Spearman correlation method shows how well two similarity matrices relate to each other by calculating correlation factor (Clarke et al., 2014). The analysis was done on BC rank similarity matrix of pigments concentrations and BC matrix of phytoplankton counts. In case RELATE analysis indicate a high correlation factor, BEST global test is run to find the subset data of one BC matrix (in our case pigment concentrations) that explains the structure of data in another BC matrix (in our case phytoplankton counts) (Clarke et al., 2014). In that way we aim to calculate which set of pigments have the highest correlation with the phytoplankton community structure.

In order to visualize the correlation between resulted pigment set and phytoplankton counts, and test its significance, LINKTREE constrained binary divisive clustering analysis and similarity profile test (SIMPROF) were run, respectively (Clarke et al., 2014). LINKTREE produces a dendrogram that shows clustering of ST1, ST2, and ST3 based on phytoplankton counts, and at the same time explains the cluster structure by showing pigment concentration thresholds that cause the main splits.

Results

Water column hydrography

The deep chlorophyll maximum layer (DCM) was defined as highest fluorescence signal encountered during station profiles. For profiles collected at ST1 and ST2, it set at ~130 m, while it was found at much shallower depths at coastal ST3 (~30 m). As expected mixed-layer depth (MLD, calculated as the depth at which density differed from the mean density in the top 10 m by < 0.05 kg m^{-3}), was sitting in proximity of the DCM, at ~ 130 m for ST1 and ST2, and at ~ 90 m depth at ST3.

Phytoplankton diversity of North Pacific ocean

The encountered phytoplankton community was mostly comprised of coccolithophores (35.5%), diatoms (25.2%) and dinoflagellates (19.5%) while cryptophytes, phytoflagellates and

silicoflagellates, etc. were included in group "other" that makes 19.8% of phytoplankton counts. A total of 207 taxa have been determined from both Niskin and net samples of which: 106 diatoms, 48 coccolithophores, 41 dinoflagellates, 7 other autotrophs, 4 heterotrophs, and 1 cyanobacterium. Cryptophytes were observed but were not identified to the genus level (Table S1). Of the 207 taxa, more than a half (113) taxa are found only in net samples: 42 diatoms, 40 coccolithophores, 27 dinoflagellates and 4 other heterotrophs.

Spatial distribution of phytoplankton groups using microscopy and pigments

Microscopy counts resulted in abundances of phytoplankton groups that indicate lower biomass of micro- and nanophytoplankton at NPSG oligotrophic ecosystem (ST1 and ST2) in comparison to eutrophic CCS (ST3). Moreover, results elucidate variable spatial distribution of microphytoplankton, while spatial distribution of nanophytoplankton is even (Fig. 2a and 2b). Diatoms of micro-fraction increased for an order of magnitude with the transition to ST3, while distribution of dinoflagellates, coccolitophores, and other phytoplankton groups of microphytoplankton stay constant across the investigated transect (Fig. 2a). Nano fraction of diatoms, dinoflagellates, and coccolitophores had even distribution across stations, while "other" cells (e.g. cryptophytes) exhibited similar behaviour to micro-scale diatoms, increasing their abundances at ST3 (Fig. 2b).

Average pigment concentrations encountered on transect (Table S4) show F_p index that is higher at ST3 (0,087), and lower at ST1 (0,018) and ST2 (0,021). Alloxanthin, zeaxanthin, divinyl chlorophyll *b* (DVChl *b*), and lutein are the pigment set with the highest correlation to phytoplankon counts, as identified by the BEST global test that resulted in Spearman correlation coefficient (Rho=0.532) with $p < 0.1\%$ significance level (Table S3). Spatial distribution of these four pigments and divinyl chlorophyll *a* (DVChl *a*) across stations elucidates two clearly distinct environments (Fig. 3a). ST1 and ST2 exhibited higher concentrations of DVChl *a* and zeaxanthin, the biomarkers for *Prochlorococcus* and *Synechococcus* (respectively), implying the cyanobacteria domination in this region. Entering ST3, concentrations of previous pigments fall substantially, while concentrations of cryptophytic biomarker alloxanthin rise. Moreover, we observed higher concentrations of 19'-hexanoyloxyfucoxanthin (19HF) and fucoxanthin (Table S4), biomarkers for coccolithophores and mostly diatoms, respectively. Biomarkers peridinin and prasinoaxanthin also dominated at ST3, representing high abundances of dinoflagellates and prasinophytes, respectively (Table S4). Furthermore, there is a strong increase of total Chl *a* concentration at ST3, when compared to oligotrophic ST1 and ST2 (Fig. 3b).

Similarity between stations and dominant taxa

Pairwise test of ANOSIM analysis displayed significant differences in phytoplankton community abundance and composition between ST1 and ST3, and ST2 and ST3 with R-value being 0.579 and 0.612, respectively (Table S2). Taxa diversity and abundances were largest at eutrophic ST3, while oligotrophic ST1 and ST2 exhibited similar community structure.

Nano-scale dinoflagellates (ESC 10-20 µm) and coccolithophores (ESC <5 µm and 5-10) contributed the most to dissimilarity of both ST1 and ST2 according to SIMPER analysis results (Table 3). Next were phytoflagellates with high contribution to the ST1 dissimilarity, while at ST2 that was *Rhizosolenia hebetata f. semispina* (Table 3). Nano-scale coccolitophorids (ESC 5-10 µm), cryptophytes and *Pseudo-nitzschia pseudodelicatissima* contributed the most to dissimilarity of ST3 (Table 3).

Dominant taxa by stations were defined as species and groups with abundance >10^4 cells L^{-1}, and the frequency of occurrence in samples >50 % (Table 2), and some of them are shown on micrographs (Figure 4). Dominant taxa present along the whole transect, but reaching highest abundances at ST3 were cryptophytes, *Gyrodinium spp*, *Nitzschia bicapitata*, nano-dinoflagellates and nano-coccolithophores (ESC <10 µm) (Table 2). On the other hand, some dominant taxa were present at only one station. Species specific to ST1 were nano-scale *Gyrodinium* sp. (ESC <20 µm), *Gymnodinium* spp., *Michaelsarsia adriaticus*, *N. braarudii*, and *Nitzschia* sp. Specific taxa at ST2 were *Calciosolenia brasiliensis*, *Nitzschia* sp. 1, *Ophiaster sp.*, and nano-coccolithophores (ESC 10-20 µm). The highest number of specific species was found at ST3, and most of them were diatoms: *Chaetoceros contortus*, *Ch. convolutus*, *Ch. debilis*, *Lennoxia faveolata*, *N. sicula*, *Proboscia alata*, *Pseudo-nitzschia pseudodelicatissima*, *Rhizosolenia hebetata f. semispina*, *R. cleveii*, *Thalassionema nitzschioides*, and nano-scale *Thalassiosira* sp. (ESC <20 µm). Other two specific taxa for ST3 were *Micromonas* sp. and *Oxytoxum cf. variabile* (ESC <20 µm) (Table 2). Highest abundance of diatoms at ST3 was recorded thanks to the high quantities of *Pseudo-nitzschia pseudodelicatissima*.

Correlation between pigments and phytoplankton counts

HPLC based pigment concentrations closly followed the significant across-transect trends observed in phytoplankton abundances, as demonstrated by the RELATE test (Fig. S1b). Alloxanthin, zeaxanthin, DVChl *b*, and lutein contributed the most to similarities in trends, as shown by the BEST global test (Table S3). A clear split between coastal, eutrophic ST3 and oligotrophic ST1 and ST2 is visible in dendogram visualising LINKTREE constrained binary divisive clustering analysis done on phytoplankton counts and pigment concentrations (Fig. 5). This primary split (Node A>B, K), that can be explained by the specific threshold of alloxanthin (-0,0089 µg/L for ST1 and ST2, 0,001 µg/L for ST3) is highly significant (SIMPROF test, Fig. S1a).

Further splits in the dendogram are driven by secondary pigments and demonstrate finer differences within the ecosystem types, on olgotrophic side lutein or zeaxantin (Node B), and on eutrophic side by zeaxantin (Node K>L, N) and further down (Node N) by the lutein. Note that only some of the splits in this dendogram are significant (black lines on the Fig. 5) according to SIMPROF test (Fig. S1a).

Discussion

Horizontal and vertical distribution of phytoplankton

Planktonic dispersal rate varies across marine planktonic taxa, while negative relationship between dispersal scale and body size causes less abundant and larger-fraction plankton (in near-surface, epipelagic waters) to have shorter dispersal scales and larger spatial species-turnover rates than the more abundant, smaller-fraction plankton (Villarino et al., 2018). The larger phytoplankton will be more similar at geographically proximate locations, and dissimilar between distant locations while it would allow smaller, more abundant phytoplankton (body size <2 mm) to travel greater distances (Finlay, 2002; Martiny et al., 2006; Villarino et al., 2018). This explains even spatial distribution of all nanophytoplankton fractions between stations, while microphytoplankton fractions, especially diatoms, are most abundant at ST3 (Fig. 3a and b). Additionally, we observed the highest number of specific diatom species at ST3 (Table 2).

Besides horizontal distribution between regions, the phytoplankton community also has a vertical distribution that was researched in a study done at the East China Sea and Yellow Sea (Kang et al., 2021). Results showed significant differences between the two depths. At oligotrophic 1 % light depth, diatoms were the dominant group, while fucoxanthin and alloxanthin showed the highest production rates. On the other hand, at eutrophic 100% light depth, cyanobacteria contributed the most, while production of all pigments was very low, except for Chl *a*. Also, Kang et al., 2021 measured environmental conditions that show oligotrophic conditions at the surface and eutrophic deep layer. Their results can be compared with the dominance of picophytoplankton, nanophytoplankton, and cyanobacteria at oligotrophic NPSG (ST1 and ST2), and the large contribution of microphytoplankton at eutrophic CCS (ST3).

Phytoplankton community structure

Microphytoplankton

Microphytoplankton abundance increased at eutrophic ST3 (Fig. 2a), where diatoms were dominant (Table 2) and contributed the most to the dissimilarity to other stations (Table 3). Similar assemblage was discussed in a study done by Iriarte & Fryxell, 1995 who researched microphytoplankton community structure at equatorial Pacific at 140°W during El Niño 1992 event. Taxa groups that contributed the most to the biomass were diatoms, dinoflagellates and coccolitophores. Dominant species during March to April were *Pseudonitzschia delicatissima*, *Thalassionema* spp., *Thalassiothrix* spp., *Thalassiosira lineata*, and *Oxytoxum variabile*. In October the same species dominated, with additional two: *Calcidiscus leptoporus* and *Chaetoceros atlanticus*. Furthermore, Yamaguchi et al., 2002 analyzed plankton of three regions in western North Pacific: subarctic, subtropical and transitional. Eutrophic subarctic region had the highest phytoplankton biomass, and community dominated with dinoflagellates and diatoms.

Eutrophic ST3 had the highest abundances of *Pseudo-nitzschia pseudodelicatissima* that was absent from ST1 and ST2. *Pseudonitzschia* taxa, while cosmopolitant (Hasle, 2002), seems to be prevalent in communities along the California coast. While no mention of the specific species in that area is found in the literature, the taxa is known to respond to the environmental drivers - both human induced and inate to the system (Parsons & Dortch, 2002). Trainer et al., 1998 found that two *Pseudo-nitzschia* species were causing sea lion die-off due to domoic acid poisoning along the central California coast, and observed that the appearance of these species coincided with upwelling zones near the coast. Others point to increased fertilizer use and agricultural run-off causing eutrophication (Smith et al., 1990). A diatom species *Lennoxia faveolata* had the second-highest abundance among diatoms at ST3 and was not detected in other stations. Thomsen et al., 1993 who first described it, found high numbers in samples from Californian waters during winter, but not much more is known about it.

Cyanobacteria

Pigments DVCHl *a*, and zeaxanthin were recorded in high concentration at oligotrophic NPSG (ST1 and ST2), that falls substantially towards eutrophic CCS (ST3), as shown by pigment analysis (Table S4, Fig. 3a). Since DVCHl *a*, and zeaxanthin are biomarkers for cyanobacteria *Prochlorococcus* and *Synechococcus*, respectively, we can conclude they reach high abundances in oligotrophic ecosystem. However, zeaxanthin concentrations were less variable throughout investigated transect, implying *Synechococcous* has adapted differently to eutrophic ecosystem. Other studies done in oligotrophic regions of the North Pacific also observed dominance of *Prochlorococcus*, followed by high abundance of *Synechococcus* (Andersen et al., 1996; Fujiki et al., 2016).

Berthelot et al., 2019 did a research at the same investigated transect and showed cyanobacteria distribution similar to ours. They analysed the inorganic carbon fixation rates, and nitrate, ammonium, and urea uptake rate at the single cell level in photosynthetic pico-eukaryotes (PPE) and *Prochlorococcus* and *Synechococcus*. The results showed that photosynthetic growth rates of *Prochlorococcus* were higher at NPSG in comparison to CCS region, while *Synechococcocus* growth rate did not show statistically significant difference between the two regions (Berthelot et al., 2019). This distribution can be caused by different physiological and photosynthetic adaptation of these two taxa to biogeochemical conditions of the ecosystem (Partensky, Hess & Vaulot, 1999a; Partensky, Blanchot & Vaulot, 1999b; Biller et al., 2014). In general, *Synechococcocus* is more ubiquitous (Campbell & Vaulot, 1993; Li, 1995; Blanchot & M, 1996; Otero, Álvarez-Salgado & Bode, 2020), and often more abundant in colder and nutrient-richer coastal waters (Biller et al., 2014), whereas *Prochlorococcus* prefers warm oligotrophic waters with temperatures >15 °C (Partensky, Blanchot & Vaulot, 1999b), and its abundance drops above 50°N (Partensky, Hess & Vaulot, 1999a). Babić et al., 2017 suggest that temperature and environmental hydrodynamics may also influence variation in the abundances, structure, and distribution of both *Prochlorococcus* and *Synechococcus* populations making them ideal indicator organisms for predicting future changes in the ecosystems caused by the global warming.

Synechococcus may also be indirectly observed using the abundance of diatom *Leptocylindrus mediterraneus* because it has a symbiont colonial protozoan *Solenicola setigera* Pavillard inside which the *Synechococcus* may reside (Buck & Bentham, 1998; Gómez, 2007). *Leptocylindrus mediterraneus* has been detected on both the ST1 and ST2, albeit with low abundance. Nevertheless, the number of cyanobacterial cells should be much higher than the number of symbionts they inhabit. Therefore, although we already detected cyanobacteria by using HPLC pigment analysis, it could be possible to use this indirect three-partner associated symbiosis as a method to record the presence of *Synechococcus*.

Coccolitophores

Coccolithophorid contribution to community composition is significant on all stations, with dominant nano- fraction, especially at greater depths. Micro-scale coccolithophores have a more significant abundance at ST1 and ST2, but they are absent at ST3. Coccolithophorid pigment proxy 19HF has a relatively high ratio on all stations when compared to other pigments. Its presence may point to the higher contribution of pico-scale coccolithophores in bigger depths at ST3. *Michaelsarsia adriaticus* was a dominant species present only at ST1, where as dominant *Calciosolenia brasiliensis* and *Ophiaster* sp. were specific to ST2. Dominant species observed on both ST1 and ST2 were *Calciosolenia murrayi* and *Discosphaera tubifera*. ST3 was dominated by nano-scale coccolithophorids (ESC <5 µm and 5-10).

Domination of coccolithophores at ST1 and ST2 point to species more adapted to oligotrophic conditions, while indirect observation of 19HF at ST3 implies a shift to the more eutrophic-adapted, smaller coccolithophores species. Li et al., 2013 observed concentrations of 19HF in the Pacific that was low in the upper euphotic zone but increased with depth. Fujiki et al., 2016 also observed low surface 19HF and 19BF concentration (< 0.5 mg/m^3) that is increasing below 70 m. This would suggest that the coccolithophores are physiologically adapted to low light, nutrient-enriched regions of the water or the 19HF came from other lineages containing the coccolithophorid-indicative marker pigment (Carreto et al., 2001; Landry, 2003).

Okada & Honjo, 1973 recorded 90 coccolitophorid species in North and Cental Pacific. Based on community structure, they described 6 zones, and Zones B (Transitional Pacific) and C (Central-North Pacific) match our sampling transect. They observed high abundance of *Emiliania huxley* (cold variety), *Rhabdosphaera clavigera*, and *Umbellosphaera irregularis*. Less abundant species present in this area were *Discosphaera tubifera*, *Syracosphaera* spp, *Rhabdosphaera stylifera*, *Umbellosphaera tenuis*, *Umbilicosphaera hulburtiana*, *Um-bilicosphaera sibogae*, which is similar community structure observed in our study (Table S1), however we observed other dominat species: *Calciosolenia brasiliensis*, *Calciosolenia murrayi*, *Discosphaera tubifera*, *Michaelsarsia adriaticus*, and *Ophiaster* sp (Table 2). Hoepffner & Haas, 1990 identified nanophytoplankton community of NPSG by using electron microscopy, and observed that Prymnesophyceae contributed the most (55%), with equal abundances of Prymnesiales and Coccosphaerales. Dominant taxa were *E.huxley*, *O. formosu*s, *R. clavigera*, and *C. murrayi*. Another study in NPSG revealed a total of 53 species, from which most abundant were *D.*

tubifera, *U. tenuis*, and *Heladosphaera cornifera* in the upper layer (0 -80 m), and *Anthosphaera oryza*, *Florisphaera profunda*, *Thorosphaera flabellata*, and *Oolithotus fragilis* in the lower layers (140-200 m) (Reid, 1980). Other frequent species observed at the surface were *Acanthoica acanthifera*, *Calyptrosphaera oblonga*, *U. irregularis*, *Rhabdosphaera stylifera*, *Syracosphaera pulchra*, and *S. pirus* (Reid, 1980). Most of listed species we detected as well (Table 2).

Phytoplankton chemotaxonomy and its relation to microscopy

Chemotaxonomy is a method that allows characterization of the phytoplankton community to coarser taxa than the microscopy can, however, offering insight into the nano- and pico-planktonic composition that is undetectable by classical microscopy methods (Kramer, Siegel & Graff, 2020). Following the decades of research in which pigment composition was related to the microscopy based one, it proved to have biases as concentrations of pigment biomarkers, and their relation to the chlorophyll a are not always the best representative of the targeted taxa (Harry Havskum et al., 2004; Irigoien et al., 2004; Pan et al., 2020). These vary with physiology of the cells, and environmental factors such as irradiance, nutrient availability, day length, temperature, and mixing status (Higgins, Wright & Schluter, 2011).

Regardless of biases, HPLC approach allowed us to track distribution of cyanobacterial taxa indirectly through their pigments proxy, DVChl *a*, and zeaxanthin, that reached their highest peak at oligotrophic ST1 and ST2. Highest concentrations of fucoxanthin, peridinin, 19HF, alloxanthin, and prasinoaxanthin were observed at ST3 (Table S4), which indicate higher abundances of diatoms, dinoflagellates, coccolitophores, cryptophytes, and prasinophytes respectively.

Claustre, 1994 proposed another use of pigments that can determine trophic state of the area by calculating the Fp index (the ratio of pigments highly correlated to changes in Chl *a* concentration to other pigments that are less variable). Study showed fucoxanthin and peridinin, biomarkers for mostly diatoms and dinoflagellates respectively, had a higher correlation with the change of total Chl *a* in comparison to other pigments, meaning rise in biomass can be correlated with diatoms and dinoflagellates growth. We used the same approach and calculated higher Fp index at ST3 in comparison to ST1 and ST2, which correlates with the rise of fucoxanthin and peridinin in CCS (Table S4).

However, four pigments that were the most important when it comes to distinguishing the community composition across the investigated transect (Fig. 3a, Table S3), were not the ones connected to dominating microflora. Alloxanthin, zeaxanthin, divinyl chlorophyll *b* (DVChl *b*), and lutein are pigments connected to “less charismatic” and elusive to microscopy nano- and pico-scale plankton, such as cryptophytes, prasinophytes, and *Prochlorococcus*. Furthermore, one interesting trend arose from LINKTREE statistical analysis, showing that pigment alloxanthin determined most the differences in phytoplankton community between the CCS and open ocean stations (Fig. 5). While the imaging-based analysis did point cryptophytes play an

important role in distinguishing two communities (Table 2), other taxa, namely cooclithophorids and diatoms also seemed to drive the ecosystem differences.

Contrasting North Pacific ecosystems

In this paper, the analyzed data showed distinct environments characterized by differences between phytoplankton abundances and concentrations of pigments along a transect that comprises an open ocean and a coast. We recorded lower phytoplankton counts at NPSG which is the largest ecosystem on the planet with reduced intake of nutrients in the euphotic zone, low primary production (PP) and export of carbon to deeper layers (Karl & Church., 2017; Kavanaugh et al., 2018). On the other hand, the phytoplankton counts were higher at the CCS that is more eutrophic ecosystem with seasonal upwellings, higher PP, and frequent blooms ("Abyssal time-series studies at Station M"; Closset et al., 2021). Furthermore, the Columbia River influences the CCS with an increased terrigenous contribution raising the trophic state(Hickey & Banas, 2008). Differences between ecosystems can also be detected by observing maximum Chl *a* concentration, and our results show that it was higher and more variable in CCS, in comparison to NPSG. High chlorophyll concentrations were already recorded in northern part of CCS (Ware & Thomson, 2005), while studies in other eutrophic ecosystems show similar trend (Zhang, Wang & Yin, 2018; Miranda-Alvarez et al., 2020). Fujiki et al., 2016 observed low Chl *a* concentration at the ALOHA station (< 0.05 mg/m^3), where as at ST1 and ST2 concentration did not exceed 0.4 µg/L.

Our results demonstrate the power of combined techniques, in this case microscopy and pigments, when exploring the ecosystem diversity (Irigoien et al., 2004). Both techniques separately managed to differentiate these two ecosystems, while each of the techniques, thanks to their strengths and biases, defined different taxonomic drivers. Going forward, our results support ongoing research to facilitate observing phytoplankton community composition from space (Kramer et al., 2019). While pigment composition, carrying colour component, can be the primary validation tool for future views of diversity from space (e.g. NASA PACE mission) (Werdell et al., 2019), it does not offer a complete view of the ecosystem diversity, or a full connection to the climate-important phytoplankton long time-series data.

Conclusions

This research shows significance of combining both microscopy and chemotaxonomy to elucidate the diversity of phytoplankton community that includes all size fractions. Having knowledge on phytoplankton biodiversity helps to predict future changes in phytoplankton community and marine ecosystem in response to changes in climate. Therefore, we are proposing more studies of large marine ecosystems such as the Pacific that will utilize advantages of both methods in order to gather data on true phytoplankton community diversity. We conclude that these data bases should be used in the future to correlate the data in conjunction with radiometry to develop algorithms and calibration of sensor technology of orbital satellites for better observation of the subtle colour differences of the oceans. Since only a small area of North Pacific has been studied in this research, it is necessary to increase

research efforts and collect data on phytoplankton community structure and its pigments in Pacific and other oceans.

Funding: This work was funded by Croatian Science Foundation under projects BIOTA (UIP-2013-11-6433) and ISLAND (IP-2020-02-9524), the Schmidt Ocean Institute, NASA GSFC Ocean Ecology Lab, and NASA's PACE mission. We thank Jorijntje Henderiks for providing financial support for SEM analyses at Uppsala University (Swedish Research Council grant 2011-4866 and other funding).

Acknowledgments: We thank the captain and crew of the R/V Falkor and the "Sea to Space" science party, who made this research possible.

References

A holistic approach to marine Eco-systems biology. 2011. *PLoS Biol* 9:7–11.

Abyssal time-series studies at Station M. *Available at https://www.mbari.org/station-m-time-series/* (accessed December 1, 2022).

Almazán-Becerril A, Rivas D, García-Mendoza E. 2012. The influence of mesoscale physical structures in the phytoplankton taxonomic composition of the subsurface chlorophyll maximum off western Baja California. *Deep Sea Research Part I: Oceanographic Research Papers* 70:91–102.

Andersen RA, Bidigare RR, Keller MD, Latasa M. 1996. A comparison of HPLC pigment signatures and electron microscopic observations for oligotrophic waters of the North Atlantic and Pacific Oceans. *Deep Sea Res* II 43:517–537.

Babić I, Petrić I, Bosak S, Mihanović H, Radić ID, Ljubešić Z. 2017. Distribution and diversity of marine picocyanobacteria community: Targeting of Prochlorococcus ecotypes in winter conditions (southern Adriatic Sea. *Mar. Genomics* 36:3–11.

Berthelot H, Duhamel S, L'Helguen S, Maguer J-F, Wang S, Cetinić I, Cassar N. 2019. NanoSIMS single cell analyses reveal the contrasting nitrogen sources for small phytoplankton. *The ISME Journal* 13:651–662. DOI: 10.1038/s41396-018-0285-8.

Biller S, Berube P, Berta-Thompson J, Kelly L, Roggensack SE, Awad L, Roache-Johnson KH, Ding H, Giovannoni SJ, Rocap G, Moore LR, Chisholm SW. 2014. Genomes of diverse isolates of the marine cyanobacterium Prochlorococcus. *Sci Data* 1:140034. DOI: 10.1038/sdata.2014.34.

Blanchot J, M R. 1996. Picophytoplankton abundance and biomass in the western tropical Pacific Ocean during the 1992 El Nino year: Results from flow cytometry. *Deep. Res. Part I Oceanogr. Res. Pap* 43:877–895.

Booth BC, Lewin J, Postel JR. 1993. Temporal variation in the structure of autotrophic and heterotrophic communities in the subarctic Pacific. *Prog. Oceanogr* 32:57-99 10 1016 0079-6611 93 90009–3.

Bray JR, Curtis JT. 2006. An Ordination of the Upland Forest Communities of Southern Wisconsin. *Ecol. Monogr* 27:325–349. DOI: 10.2307/1942268.

Buck KR, Bentham WN. 1998. A novel symbiosis between a cyanobacterium, Synechococcus sp., an aplastidic protist, Solenicola setigera, and a diatom, Leptocylindrus mediterraneus, in the open ocean. *Mar. Biol* 132:349–355.

Cael BB, Dutkiewicz S, Henson S. 2021. Abrupt shifts in 21st-century plankton communities. *Science Advances* 7:eabf8593. DOI: 10.1126/sciadv.abf8593.

Campbell L, Vaulot D. 1993. Photosynthetic picoplankton community structure in the subtropical North Pacific Ocean near Hawaii (station ALOHA. *Deep. Res. Part I* 40:2043–2060.

Carreto JI, Seguel M, Montoya NG, Clément A, Carignan MO. 2001. Pigment profile of the ichthyotoxic dinoflagellate Gymnodinium sp. from a massive bloom in southern Chile. *J. Plankton Res* 23:1171–1175.

Clarke KR. 1993. Non-parametric multivariate analyses of changes in community structure. *Aust. J. Ecol* 18:117-143 10 1111 1442-9993 1993 00438.

Clarke KR, Gorley RN, Somerfield PJ, Warwick RM. 2014. *Change in marine communities: an approach to statistical analysis and interpretation*. PRIMER-E: Plymouth.

Claustre H. 1994. The trophic status of various oceanic provinces as revealed by phytoplankton pigment signatures. *Limnology and Oceanography* 39. DOI: 10.4319/lo.1994.39.5.1206.

Closset I, McNair HM, Brzezinski MA, Krause JW, Thamatrakoln K, Jones JL. 2021. Diatom response to alterations in upwelling and nutrient dynamics associated with climate forcing in the California Current System. *Limnology and Oceanography* 66:1578–1593. DOI: https://doi.org/10.1002/lno.11705.

Finlay BJ. 2002. Global dispersal of free-living microbial eukaryote species. *Science* 296:1061–1063.

Fujiki T, Sasaoka K, Matsumoto K, Wakita M, Mino Y. 2016. Seasonal variability of phytoplankton community structure in the subtropical western North Pacific. *Journal of Oceanography* 72:343–358.

Gómez F. 2007. The consortium of the protozoan Solenicola setigera and the diatom Leptocylindrus mediterraneus in the Pacific Ocean. *Acta Protozool* 46:15–24.

Havskum H., Schlüter L., Scharek R., Berdalet E., Jacquet S. 2004. Routine quantification of phytoplankton groups- microscopy or pigment analyses? *Marine Ecology Progress Series* 273:31–42.

Hasle GR. 2002. Are most of the domoic acid-producing species of the diatom genus Pseudo-nitzschia cosmopolites? *Harmful Algae* 1:137–146. DOI: https://doi.org/10.1016/S1568-9883(02)00014-8.

Hickey B, Banas N. 2008. Why is the Northern End of the California Current System So Productive? *Oceanography* 21:90–107.

Higgins HW, Wright SW, Schluter L. 2011. Quantitative interpretation of chemotaxonomic pigment data. In: Roy S, Llewellyn CA, Egeland ES, Johansen AM eds. *Phytoplankton Pigments: Characterization, Chemotaxonomy and Applications in Oceanography*. Cambridge University Press, 257–313.

Hoepffner N, Haas LW. 1990. Electron microscopy of nanoplankton from the North Pacific central gyre. *Journal of Phycology* 26:421–439. DOI: 10.1111/j.0022-3646.1990.00421.x.

Hooker SB, Clementson L, Thomas CS, Schlüter L, Allerup M, Ras J, Claustre H, Normandeau C, Cullen J, Kienast M. 2012. The Fifth SeaWiFS HPLC Analysis Round-Robin Experiment (SeaHARRE–5. In: *NASA Technical Memorandum 2012–217503*. Greenbelt, MD: NASA Goddard Space Flight Center,.

Iriarte JL, Fryxell GA. 1995. Micro-phytoplankton at the equatorial Pacific (140°W) during the JGOFS EqPac Time Series studies: March to April and October 1992. *Deep Sea Research Part II: Topical Studies in Oceanography* 42:559–583. DOI: https://doi.org/10.1016/0967-0645(95)00031-K.

Irigoien X, Meyer B, Harris R, Harbour D. 2004. Using HPLC pigment analysis to investigate phytoplankton taxonomy: the importance of knowing your species. *Helgoland Marine Research* 58:77–82. DOI: 10.1007/s10152-004-0171-9.

Kammerer JC. 1987. Largest Rivers in the United States (Water Fact Sheet. *US Geological Survey Fact Sheet OFR*:87–242. DOI: 10.3133/OFR87242.

Kang J, Kim Y, Lee CH, Yoo H, Jang HK, Kim MJ, Lee SH. 2021. Vertical distribution of phytoplankton community and pigment production in the Yellow Sea and the East China Sea during the late summer season. *Water*.

Karl DM, Church. MJ. 2017. Ecosystem Structure and Dynamics in the North Pacific Subtropical Gyre: New Views of an Old Ocean. *Ecosystem* 20:433-457 10 1007 10021-017-0117–0.

Kavanaugh MT, Church MJ, Davis CO, Karl DM, Letelier RM, Doney SC. 2018. ALOHA From the Edge: Reconciling Three Decades of in Situ Eulerian Observations and Geographic Variability in the North Pacific Subtropical Gyre. *Frontiers in Marine Science* 5:130. DOI: 10.3389/fmars.2018.00130.

Kodama T, Watanabe T, Taniuchi Y, Kuwata. A, Hasegawa. D. 2021. Micro-size plankton abundance and assemblages in the western North Pacific Subtropical Gyre under microscopic observation. *PLoS ONE* 16:0250604.

Kramer SJ, Siegel DA, Chase AP, Kramer SJ, Haëntjens N, Boss ES, Karp-Boss L, Edmondson M, Graff JR. 2019. How can phytoplankton pigments be best used to characterize surface ocean phytoplankton groups for ocean color remote sensing algorithms? *Journal of Geophysical Research: Oceans* 124:7557-7574 ,.

Kramer SJ, Siegel DA, Graff JR. 2020. Phytoplankton Community Composition Determined From Co-variability Among Phytoplankton Pigments From the NAAMES Field Campaign. *Frontiers in Marine Science* 7. DOI: 10.3389/fmars.2020.00215.

Kramer SJ, Siegel DA, Maritorena S, Catlett D. 2022. Modeling surface ocean phytoplankton pigments from hyperspectral remote sensing reflectance on global scales. *Remote Sensing of Environment* 270:112879. DOI: https://doi.org/10.1016/j.rse.2021.112879.

Kudela RM, Horner-Devine AR, Banas NS, Hickey BM, Peterson TD, McCabe RM, Lessard EJ, Frame E, Bruland KW, Jay DA, Peterson JO, Peterson WT, Kosro PM, Palacios SL, Lohan MC, Dever EP. 2010. Multiple trophic levels fueled by recirculation in the Columbia River plume. *Geophys. Res. Lett* 37:1–7.

Landry MR. 2003. Phytoplankton growth and microzooplankton grazing in high-nutrient, low-chlorophyll waters of the equatorial Pacific: Community and taxon-specific rate assessments from pigment and flow cytometric analyses. *J. Geophys. Res* 108.

Li WK. 1995. Composition of ultraphytoplankton in the central north Atlantic. *Mar. Ecol. Prog. Ser* 122:1–8.

Li B, Karl DM, Letelier RM, Bidigare RR, Church MJ. 2013. Variability of chromophytic phytoplankton in the North Pacific Subtropical Gyre. *Deep. Res. Part II Top. Stud. Oceanogr* 93:84–95.

Longhurst A. 2007. *Ecological Geography of the Sea Longhurst*. Boston, MA: Academic Press.

Martiny JBH, Bohannan BJM, Brown JH, Colwell RK, Fuhrman JA, Green JL, Horner-Devine MC, Kane M, Krumins JA, Kuske CR, Morin PJ, Naeem S, Øvreås L, Reysenbach AL, Smith VH, Staley JT. 2006. Microbial biogeography: Putting microorganisms on the map. *Nat. Rev. Microbiol* 4:102–112.

McQuatters-Gollop A, Johns D, Bresnan E, Skinner J, Rombouts I, Stern R, Aubert A, Johansen M, Bedford J, Knights A. 2017. From microscope to management: The critical value of plankton taxonomy to marine policy and biodiversity conservation. *Marine Policy* 83:1–10. DOI: 10.1016/j.marpol.2017.05.022.

Miranda-Alvarez C, González-Silvera A, Santamaría-del-Angel E, López Calderón J, Godínez VM, Sánchez Velasco L, Hernández Walls R. 2020. Phytoplankton pigments and

community structure in the northeastern tropical pacific using HPLC-CHEMTAX analysis. *J. Oceanogr* 76:91–108.

Moore JK, Fu W, Primeau F, Britten GL, Lindsay K, Long M, Doney SC, Mahowald N, Hoffman F, Randerson JT. 2018. Sustained climate warming drives declining marine biological productivity. *Science* 359:1139–1143. DOI: 10.1126/science.aao6379.

Morgan CA, De Robertis A, Zabel RW. 2005. Columbia River plume fronts. I. Hydrography, zooplankton distribution, and community composition. *Mar. Ecol. Prog. Ser* 299:19–31. DOI: 10.3354/meps299019.

Okada H, Honjo S. 1973. The distribution of oceanic coccolithophorids in the Pacific. *Deep Sea Research and Oceanographic Abstracts* 20:355–374. DOI: https://doi.org/10.1016/0011-7471(73)90059-4.

Olson RJ, Sosik HM. 2007. A submersible imaging-in-flow instrument to analyze nano- and microplankton: Imaging FlowCytobot. *Limnol. Oceanogr.: Methods* 5:195–203.

Otero J, Álvarez-Salgado XA, Bode A. 2020. Phytoplankton Diversity Effect on Ecosystem Functioning in a Coastal Upwelling System. *Frontiers in Marine Science* 7:959.

Pal R, Choudhury AK. 2014. An Introduction to Phytoplanktons: Diversity and Ecology.

Pan H, Li A, Cui Z, Ding D, Qu K, Zheng Y, Lu L, Jiang T, Jiang T. 2020. A comparative study of phytoplankton community structure and biomass determined by HPLC-CHEMTAX and microscopic methods during summer and autumn in the central Bohai Sea, China. *Marine Pollution Bulletin* 155:111172.

Parsons ML, Dortch Q. 2002. Sedimentological evidence of an increase in Pseudo-nitzschia (Bacillariophyceae) abundance in response to coastal eutrophication. *Limnol. Oceanogr* 47:551–558.

Partensky F, Blanchot J, Vaulot D. Differential distribution and ecology of Prochlorococcus and Synechococcus in oceanic waters: a review. *Bull. l'Institut Oceanogr. Monaco* 1999b:457–475.

Partensky F, Hess WR, Vaulot D. Prochlorococcus, a Marine Photosynthetic Prokaryote of Global Significance. *Microbiol. Mol. Biol. Rev* 1999a, 63:106–127.

Peterson W, Bond N, Robert MP, Sidney. 2016. The Blob (Part Three): Going, going, gone? 24:46–48.

Picheral M, Guidi L, Stemmann L, Karl DM, Iddaoud G, Gorsky G. 2010. The Underwater Vision Profiler 5: An advanced instrument for high spatial resolution studies of particle size spectra and zooplankton. *Limnol. Oceanogr.: Methods* 8:462–473.

Ramond P, Siano R, Schmitt S, deVargas C, Marié L, Memery. L, Sourisseau M. 2021. Phytoplankton taxonomic and functional diversity patterns across a coastal tidal front. *Sci Rep* 11:2682. DOI: 10.1038/s41598-021-82071-0.

Reid FMH. 1980. Coccolithophorids of the North Pacific Central Gyre with Notes on Their Vertical and Seasonal Distribution. *Micropaleontology* 26:151. DOI: 10.2307/1485436.

Roy S, Llewellyn CA, Egeland ES, Pigments JGP. 2011. *Characterization, Chemotaxonomy and Applications in Oceanography*. Cambridge University Press.

Smith JC, Cormier R, Worms J, Bird CJ, Quilliam MA, Pocklington R, Angus R, Hanic L. 1990. Toxic Blooms of the Domoic Acid Containing Diatom Nitzschia pungens in the Cardigan River, Prince Edward Island, in 1988. *Toxic Mar. Phytoplankt*:227–232.

Steele JH, Thorpe SA, Turekian KK. 2008. *Encyclopedia Of Ocean Sciences*. Academic Press.

Thomas MK, Kremer CT, Klausmeier CA, E L. 2012. A global pattern of thermal adaptation in marine phytoplankton. *Science* 338:1085–1088.

Thomsen HA, Buck KR, Marino D, Sarno D, Hansen LE, Osergaard JB, Krupp J. 1993. *Lennoxia faveolata gen. et sp. nov*. California: Diatomophyceae) from South America

Trainer VL, Adams NG, Bill BD, Stehr CM, Wekell JC, Moeller P, Busman M, Woodruff D. 1998. Domoic acid production near California coastal upwelling zones. *Oceanogr* 45:1818–1833.

Utermöhl H. 1958. Zur Vervollkommnung der quantitativen Phytoplankton-Methodik (Towards a perfection of quantitative phytoplankton methodology. *Mitt. int. Ver. theor. angew. Limnol* 9:1–38.

Villarino E, Watson JR, Jönsson B, Gasol JM, Salazar G, Acinas SG, Estrada M, Massana R, Logares R, Giner CR, Pernice MC, Olivar MP, Citores L, Corell J, Rodríguez-Ezpeleta N, Acuña JL, Molina-Ramírez A, González-Gordillo JI, Cózar A, Martí E, Cuesta JA, Agustí S, Fraile-Nuez E, Duarte CM, Irigoien X, Chust. G. 2018. Large-scale ocean connectivity and planktonic body size. *Nat. Commun* 9, 142:10 1038 41467-017-02535–8.

Ware DM, Thomson RE. 2005. *Bottom-Up Ecosystem Trophic Dynamics Determine Fish Production in the Northeast Pacific*. American Association for the Advancement of Science.

Watson JR, Hays CG, Raimondi PT, Mitarai S, Dong C, Mcwilliams JC, Blanchette CA, Caselle JE, Siegel DA. 2011. Currents connecting communities: Nearshore community similarity and ocean circulation. *Ecology* 92:1193-1200 10 1890 10-1436 1.

Werdell PJ, Behrenfeld MJ, Bontempi PS, Boss E, Cairns B, Davis GT, Franz BA, Gliese UB, Gorman ET, Hasekamp O, Knobelspiesse KD, Mannino A, Martins JV, McClain CR, Meister G, Remer LA. 2019. The Plankton, Aerosol, Cloud, ocean Ecosystem (PACE)

mission: Status, science, advances. *Bull. Amer. Meteor. Soc* 100:1775-1794,. DOI: 10.1175/BAMS-D-18-0056.1.

Yamaguchi A, Watanabe Y, Ishida H, Harimoto T, Furusawa K, Suzuki S, Ishizaka J, Ikeda T, Takahashi MM. 2002. Structure and size distribution of plankton communities down to the greater depths in the western North Pacific Ocean. *Deep Sea Research Part II: Topical Studies in Oceanography* 49:5513–5529. DOI: https://doi.org/10.1016/S0967-0645(02)00205-9.

Yoon J-E, Kim I-N. 2020. Climate-driven phytoplankton community shifts in the North Pacific Subtropical Gyre. In: *EGU General Assembly Conference Abstracts*. EGU General Assembly Conference Abstracts. 6754.

Zhang Y, Wang X, Yin K. 2018. Spatial contrast in phytoplankton, bacteria and microzooplankton grazing between the eutrophic Yellow Sea and the oligotrophic South China Sea. *J. Ocean. Limnol* 36:92-104 10 1007 00343-018-6259-.

Figure 1

Cruise track of the Sea to Space cruise (black line), showing approximate position of Station 1, Station 2, and Station 3.

Cruise track is superimposed onto the MODIS Aqua Chlorophyll averages for the month of February (2002-2017 average).

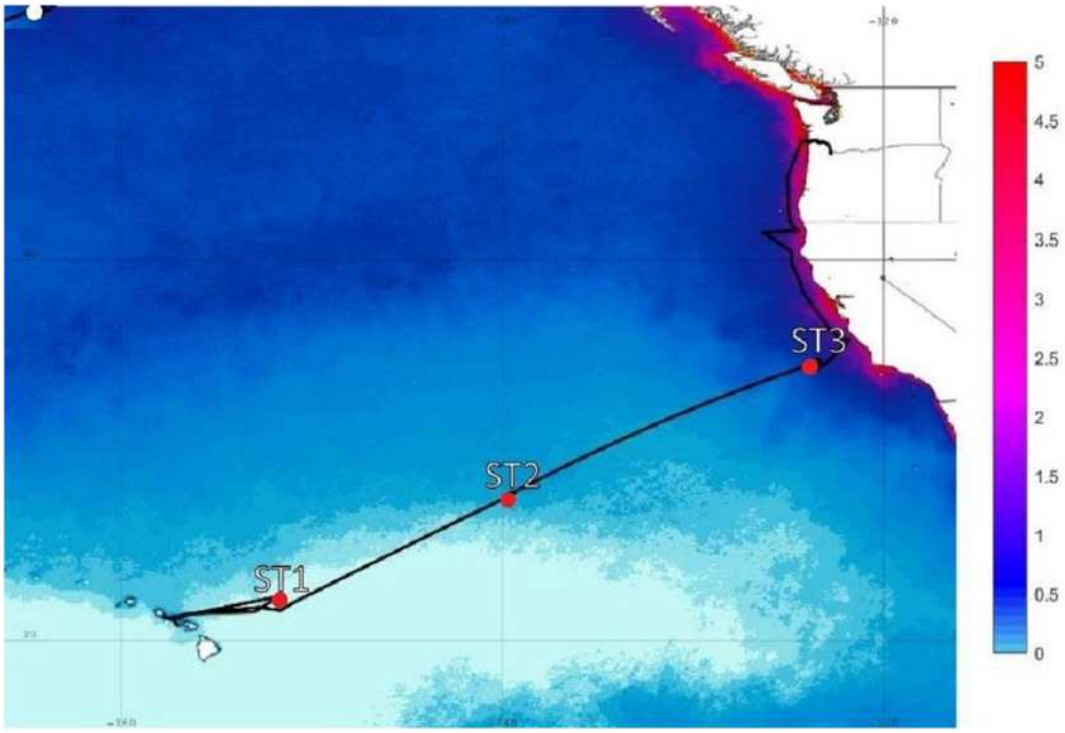

Figure 1. Cruise track of the Sea to Space cruise (black line), showing approximate position of Station 1, Station 2, and Station 3, superimposed onto the MODIS Aqua Chlorophyll averages for the month of February (2002-2017 average).

Figure 2

Spatial distribution of phytoplankton along the sampling transect in North Pacific.

(A) microphytoplankton fraction. (B) nanophytoplankton fraction. Stations (Station 1, Station 2, and Station 3) with sampling sites as CTD casts and corresponding depth (the surface layer (S), deep chlorophyll maximum (DCM), and mixed layer depth (MLD)) are shown on x-axis. Abundances (cellsL^{-1}) of diatoms, dinoflagellates, coccolithophores, and others are shown on y-axis.

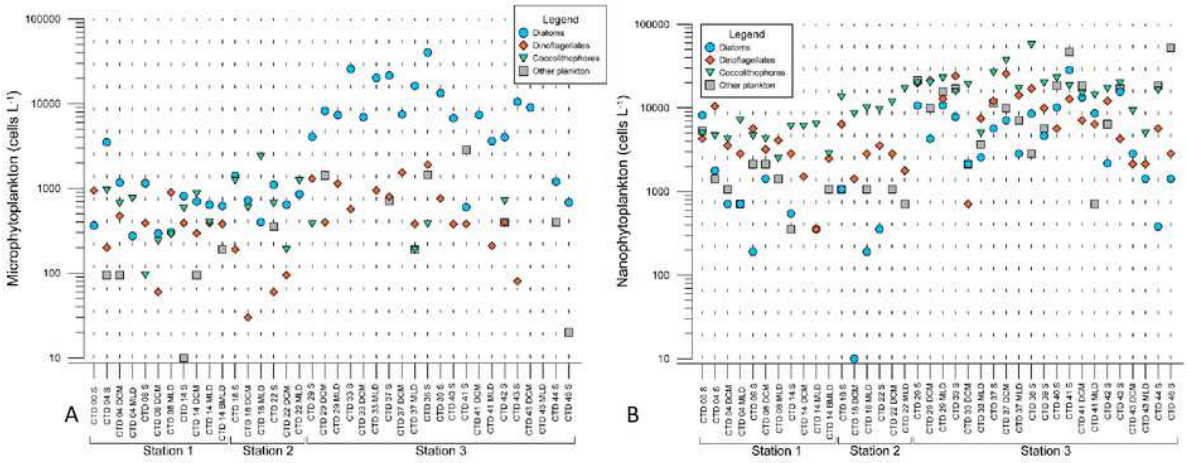

Figure 2. Spatial distribution of phytoplankton along the sampling transect in North Pacific: (a) microphytoplankton fraction; (b) nanophytoplankton fraction. Stations (Station 1, Station 2, and Station 3) with sampling sites as CTD casts and corresponding depth (the surface layer (S), deep chlorophyll maximum (DCM), and mixed layer depth (MLD)) are shown on x-axis. Abundances (cellsL-1) of diatoms, dinoflagellates, coccolithophores, and others are shown on y-axis.

Figure 3

Spatial distribution of pigments along the sampling transect in North Pacific.

(A) Pigments that correlated the most with the phytoplankton abundances: alloxanthine, zeaxanthin, divinyl chlorophyll *a* (DVChl *a*), divinyl chlorophyll *b* (DVCHl *b*), and lutein. (B) Total chlorophyll *a* (Chl *a*). Stations (Station 1, Station 2, and Station 3) with sampling sites as CTD casts and corresponding depths (the surface layer (S), deep chlorophyll maximum (DCM), and mixed layer depth (MLD)) are shown on x-axis. Concentrations of pigments (μL^{-1}) are shown on y-axis (log-scale at (A))

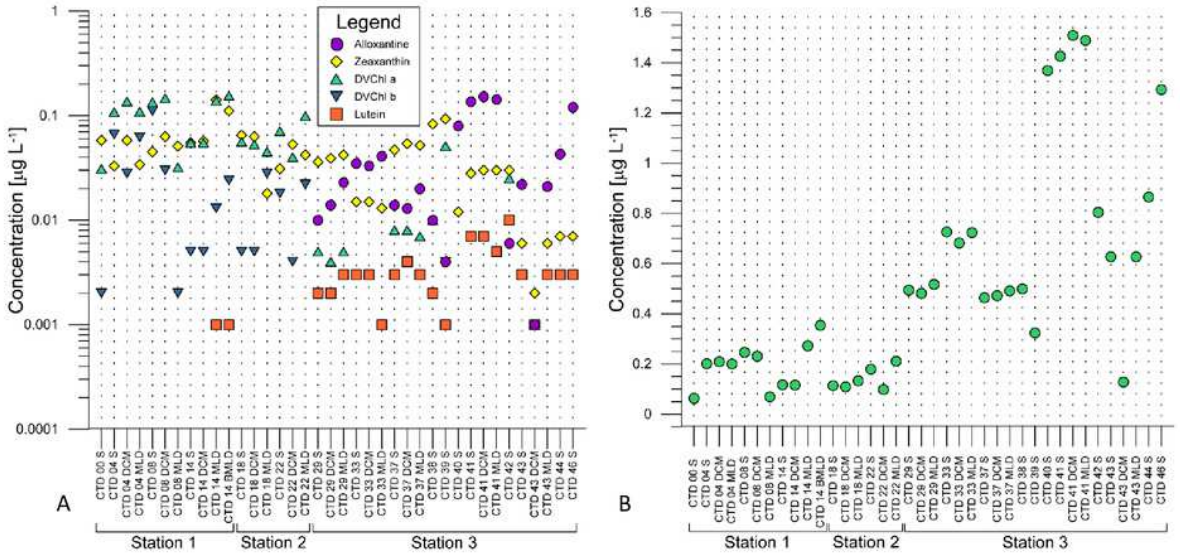

Figure 3. Spatial distribution of pigments along the sampling transect in North Pacific: (a) pig-ments that correlated the most with the phytoplankton abundances: alloxanthine, zeaxanthin, divinyl chlorophyll a (DVChl a), divinyl chlorophyll b (DVCHl b), and lutein; (b) total chloro-phyll a (Chl a). Stations (Station 1, Station 2, and Station 3) with sampling sites as CTD casts and corresponding depth (the surface layer (S), deep chlorophyll maximum (DCM), and mixed layer depth (MLD)) are shown on x-axis. Concentrations of pigments (µL-1) are shown on y-axis (log-scale at (a)).

Figure 4

Micrographs of dominant species at Station 1 (ST1), Station 2 (ST2) and Station 3 (ST3).

From top left to bottom right: *Chaetoceros convolutus* (ST3), *Rhizosolenia clevei* with *Richelia intracelularis* (arrow, ST3), *Nitzschia longissima* (ST1), *Thalassiosira* sp. (ST3), *Ophiaster* sp. (ST2), Cryptophyta (ST3), Phytoflagellates (ST1), *Chaetoceros debilis* (ST3), *Thalassionema nitzschioides* (ST3), *Michaelsarsia adriaticus* (ST1), *Nitzschia bicapitata* (ST3), *Discosphaera tubifera* (ST2).

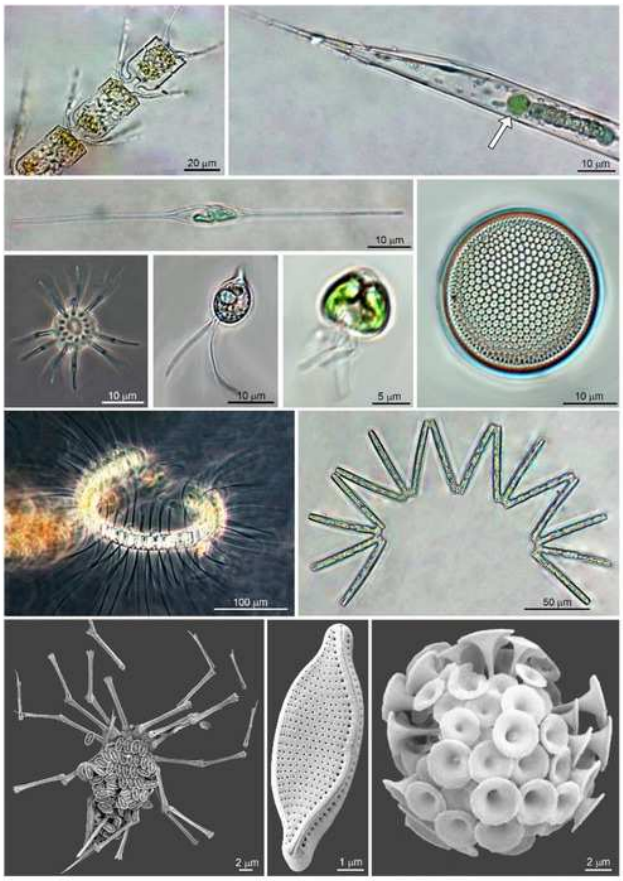

Figure 4. Micrographs of dominant species at Station 1 (ST1), Station 2 (ST2) and Station 3 (ST3). From top left to bottom right: *Chaetoceros convolutus* (ST3), *Rhizosolenia clevei* with *Richelia intracelularis* (arrow, ST3), *Nitzschia longissima* (ST1), *Thalassiosira* sp. (ST3), *Ophiaster* sp. (ST2), Cryptophyta (ST3), Phytoflagellates (ST1), *Chaetoceros debilis* (ST3), *Thalassionema nitzschioides* (ST3), *Michaelsarsia adriaticus* (ST1), *Nitzschia bicapitata* (ST3), *Discosphaera tubifera* (ST2).

Figure 5

LINKTREE binary divisive clustering analysis of the phytoplankton community at 37 sites.

Each split is constrained by a threshold of one of four best correlated pigments: alloxanthin (Allo), zeaxanthin (Zea), divinyl Chl b (DVChl b), and lutein (Lut). The first in-equality indicates sites to the left side of the split, the second sites to the right. The primary split is marked with A. Clusters marked with red dotted line are not significant by SIMPROF test. Split results: A->B,K Allo < -8,89E+03 (>0,001); B->C Lut < -8,89E+03 (>0,001) or Zea <0,065 (>0,111); K->L,N Zea <0,007 (>0,012); N->O Lut <0,007 (>0,01)

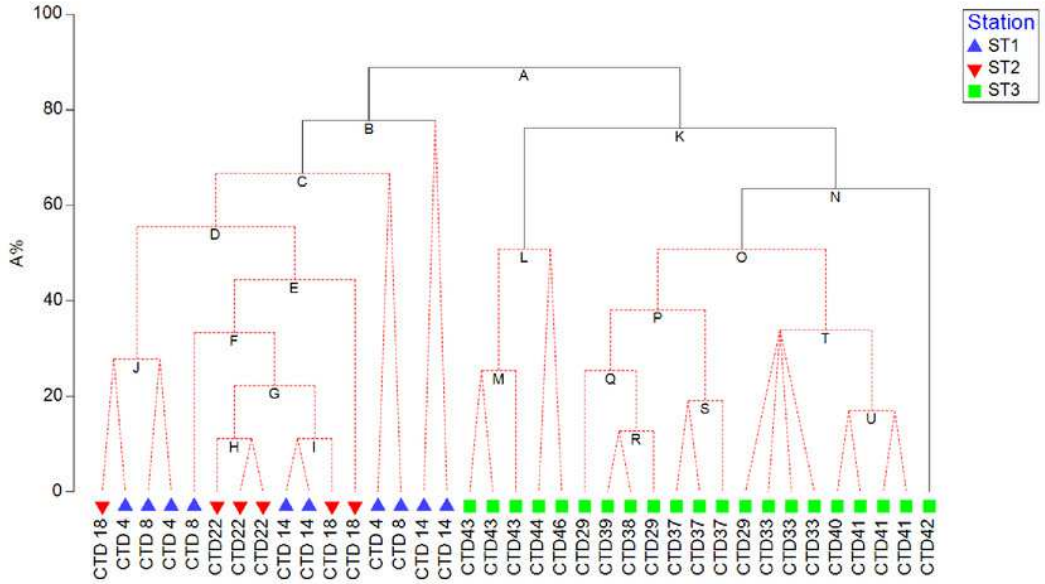

Figure 5. LINKTREE binary divisive clustering analysis of the phytoplankton community at 37 sites for which each split is constrained by a threshold of one of four best correlated pigments: alloxanthin (Allo), zeaxanthin (Zea), divinyl Chl *b* (DVChl b), and lutein (Lut). The first in-equality indicates sites to the left side of the split, the second sites to the right. The primary split is marked with A. Clusters marked with red dotted line are not significant by SIMPROF test. Split results: A->B,K Allo < -8,89E+03 (>0,001); B->C Lut < -8,89E+03 (>0,001) or Zea <0,065 (>0,111); K->L,N Zea <0,007 (>0,012); N->O Lut <0,007 (>0,01).

Table 1(on next page)

Sampling sites within each station: Station 1 (ST1), Station 2 (ST2), and Station 3 (ST3).

CTD casts, corresponding depths and water column layers are shown for each site, as well as which sample type is taken (+). Abbreviations: PHYTO (samples taken for light microscopy and pigment analyses); SEM (samples taken for scanning electron microscopy); NET (samples taken with phytoplankton net with 20µm mash size).

Table 1. Sampling sites within each station: Station 1 (ST1), Station 2 (ST2), and Station 3 (ST3). CTD casts, corresponding depths and water column layers are shown for each site, as well as which sample type is taken (+). Abbreviations: PHYTO (samples taken for light microscopy and pigment analyses); SEM (samples taken for scanning electron microscopy); NET (samples taken with phytoplankton net with 20µm mash size).

Station	Sampling site (latitude; longitude)	CTD Cast	Depth	Water column layer	PHYTO	SEM	NET
Station 1	22°14.6892; -151°52.2906	CTD4	0	S	+	+	
		CTD4	115	DCM	+	+	
		CTD4	130	MLD	+	+	
	22°16.5251; -151°44.8940	CTD8	0	S	+	+	
		CTD8	115	DCM	+	+	
		CTD8	125	MLD	+	+	+
	22°16.5251; -151°44.8940	CTD14	0	S	+	+	+
		CTD14	88	DCM	+	+	+
		CTD14	128	MLD	+	+	+
		CTD14	180	BMLD	+		
Station 2	27°42.5971; -139°29.9381	CTD18	0	S	+	+	+
		CTD18	98	DCM	+	+	+
		CTD18	128	MLD	+	+	+
	27°39.6715; -139°33.0614	CTD19	130	MLD		+	
		CTD19	composite				+
	27°42.0327; -139°41.7295	CTD21	0	S	+	+	
	27°44.7694; -139°40.2311	CTD22	0	S	+	+	+
		CTD22	95	DCM	+	+	+
		CTD22	120	MLD	+	+	+
Station 3	34°34.1060; -123°30.6151	CTD29	0	S	+	+	
		CTD29	31	DCM	+	+	
		CTD29	42	MLD	+	+	
		CTD29	composite				+
	34°31.5869; -123°33.9840	CTD33	0	S	+	+	
		CTD33	27	DCM	+	+	
		CTD33	30	MLD	+	+	
		CTD33	composite				+
	34°18.2352; -123°32.4584	CTD37	0	S	+	+	
		CTD37	2	DCM	+	+	
		CTD37	38	MLD	+	+	
		CTD37	composite				+
	34°30.011; -123°11.1985	CTD38	0	S	+	+	+
	34°54.3259; -122°41.4444	CTD39	0	S	+	+	+
	35°40.1678; -121°55.7237	CTD40	0	S	+	+	+
	35°58.2849; -122°13.5212	CTD41	0	S	+	+	+

	CTD41	14	DCM	+		
	CTD41	27	MLD	+	+	
	CTD41	composite				+
41°28.4439; -126°18.8841	CTD42	0	S	+	+	+
41°30.6406; -125°20.7072	CTD43	0	S	+	+	+
	CTD43	80	DCM	+	+	+
	CTD43	90	MLD	+	+	+
	CTD43	composite				+
41°32.8395; -124°24.2721	CTD44	0	S	+	+	+
41°32.8395; -124°24.2722	CTD46	0	S	+	+	+

Table 2 (on next page)

Maximum abundances (cells L^{-1}), and frequencies (%) for dominant species at Station 1 (ST1), Station 2 (ST2) and Station 3 (ST3).

Dominance is defined as frequency of appearance in samples >50 %. Blank cells are values that could not be determined because there were less than 40 cells in 1 L.

Table 2. Maximum abundances (cells L^{-1}), and frequencies (%) for dominant species (where dominance is defined as frequency of appearance in samples >50 %) at Station 1 (ST1), Station 2 (ST2) and Station 3 (ST3). Blank cells are values that could not be determined because there were less than 40 cells in 1 L.

Dominant Taxa/Group	Max (ST1)	Fr (ST1)	Max (ST2)	Fr (ST2)	Max (ST3)	Fr (ST3)
Chaetoceros contortus					2660	63
Chaetoceros convolutus					5320	88
Chaetoceros debilis					2660	50
Chaetoceros perpusillus	380	60	380	75		
Lennoxia faveolata					14200	69
Leptocylindrus mediterraneus	190	60	380	63		
Nitzschia bicapitata	710	50	1420	63	4260	56
Nitzschia braarudii	190	50				
Nitzschia longissima	285	60			3800	94
Nitzschia sicula					760	50
Nitzschia sp.	570	60				
Nitzschia sp. 1			285	50		
Proboscia alata					380	50
Pseudo-nitzschia pseudodelicatissima					22420	100
Rhizosolenia hebetata f. semispina					1900	88
Rhizosolenia cleveii					1140	75
Thalassionema nitzschioides					1900	50
Thalassiosira sp. (<20 µm)					8520	69
Unknown diatoms (<20 µm)	1420	50			10650	63
Gymnodinium spp.	380	50				
Gyrodinium spp.	710	60	190	63	1140	81
Gyrodinium spp. (<20 µm)	3550	50				
Oxytoxum cf. variabile (<20 µm)					2130	50
N.D. dinoflagellates (5-10 µm)	1420	70	2130	63	19880	50
N.D. dinoflagellates (10-20 µm)	2840	100	4615	100	19880	88
Calciosolenia brasiliensis			380	63		
Calciosolenia murrayi	570	50	760	88		
Discosphaera tubifera	570	50	760	88		
Michaelsarsia adriaticus	190	60				
Ophiaster sp.			950	50		
N.D. coccolithophorids (<5µm)	3550	90	7810	100	24140	88
N.D. coccolithophorids (5-10 µm)	4615	100	8520	100	29820	100
N.D. coccolithophorids (10 - 20 µm)			3195	100		
Cryptophyceae	1065	70	1065	75	32660	100
Micromonas sp.					2840	50
Phytoflagellates	1065	80			8520	75

Table 3 (on next page)

Similarities percentage (SIMPER) analysis for each taxon/group by stations.

Blank cells are values that could not be determined because there were less than 40 cells in 1L. Taxa with similarity contribution < 2 have been excluded from this table. Abbreviations: average contribution/standard deviation (δ/σ), species contribution (Σδ%).

Table 3. Similarities percentage (SIMPER) analysis for each taxon/group by stations. Blank cells are values that could not be determined because there were less than 40 cells in 1L. Taxa with similarity contribution < 2 have been excluded from this table. Abbreviations: average contribution/standard deviation (δ/σ), species contribution (Σδ%).

Taxon/Group	Station 1 (δ/σ, Σδ%)	Station 2 (δ/σ, Σδ%)	Station 3 (δ/σ, Σδ%)
Undetermined dinoflagellates (10-20 µm)	5.44, 13.84	8.06, 12.37	1.64, 7.41
Undetermined coccolitophorids (<5 µm)	1.79, 12.09	6.72, 14.02	1.67, 7.81
Cryptophyceae	0.91, 5.75	1.02, 5.60	4.97, 9.02
Gyrodinium spp.	0.65, 2.50	0.70, 2.05	1.26, 4.02
Nitzschia bicapitata	0.52, 2.50	0.68, 2.45	0.65, 2.10
Chaetoceros perpusillus	0.61, 2.39	1.03, 3.22	
Undetermined dinoflagellates (5-10 µm)	0.91, 6.13	0.72, 4.30	
Leptocylindrus mediterraneus	0.66, 2.02	0.72, 2.05	
Undetermined coccolitophorids (5-10 µm)	8.47, 15.61		6.40, 10.06
Nitzschia longissimi	0.67, 2.33		2.17, 5.41
Phytoflagellates	1.24, 7.61		1.06, 4.63
Undetermined pennate diatoms (<20 µm)	0.53, 2.36		0.75, 3.16
Nitzschia sp.	0.67, 2.06		
Michelsarsia adriatica	0.63, 2.37		
Gyrodinium spp. (<20 µm)	0.53, 2.54		
Gymnodinium spp.	0.52, 2.67		
Undetermined coccolithophorids (10-20 µm)		7.43, 12.20	
Discosphaera tubifera		1.64, 6.67	
Calciosolenia murrayi		1.55, 5.87	
Calciosolenia brasiliensis		0.72, 2.99	
Rhizosolenia hebetata f. semispina		7.34, 14.73	1.60, 3.52
Pseudo-nitzschia pseudodelicatissima			6.14, 7.62
Chaetoceros convolutes			1.61, 4.93
Rhizosolenia cleveii			1.03, 2.68
Lennoxia faveolata			0.88, 3.84
Thalassiosira (<20 µm)			0.88, 3.83
Chaetoceros contortus			0.74, 2.21